tvst

Retina

Ultra-Widefield Swept-Source Optical Coherence Tomography Angiography in the Assessment of Choroidal Changes in Young Adults With Myopia

Jian Gao[1,*], Cai-hua Rao[1,*], Fang Li[1], Lun Liu[1], and Ke-jun Liu[2]

[1] Department of Ophthalmology, The First Affiliated Hospital of Anhui Medical University, Hefei, Anhui, China
[2] Department of Ophthalmology, Dong Cheng District of The First Affiliated Hospital of Anhui Medical University, Hefei, Anhui, China

Correspondence: Jian Gao, Department of Ophthalmology, The First Affiliated Hospital of Anhui Medical University, Science Research & Teaching Building, 4th Floor, No. 218, Jixi Road, Shushan District, Hefei, Anhui 230022, China.
e-mail: shuijinglovegj@126.com

Received: September 9, 2022
Accepted: November 13, 2022
Published: December 29, 2022

Keywords: SS-OCT; choroid; myopia

Citation: Gao J, Rao C, Li F, Liu L, Liu K. Ultra-widefield swept-source optical coherence tomography angiography in the assessment of choroidal changes in young adults with myopia. Transl Vis Sci Technol. 2022;11(12):14, https://doi.org/10.1167/tvst.11.12.14

Purpose: To evaluate choroidal changes in young adults with myopia using ultra-widefield swept-source optical coherence tomography angiography (SS-OCTA).

Methods: This study enrolled 105 eyes of 105 participants who underwent SS-OCTA imaging (24 mm × 20 mm) centered on the fovea. Eyes were categorized as low myopia, moderate myopia, or high myopia. Choroidal thickness, choroidal capillary plexus (CCP) vessel density, and choroidal Sattler's and Haller's layer (CSHL) vessel density were analyzed in nine grids using built-in angiography analysis software.

Results: A significant decrease in choroidal thickness was found in most grids ($P < 0.01$) in high myopia. The CSHL vessel density also showed a significant decrease in most grids ($P < 0.05$) in high myopia. Choroidal thickness was negatively correlated with axial length in most grids ($P < 0.05$). Choroidal thinning was most evident in the macular grid ($\beta = -22.55$, $P < 0.001$). CSHL vessel density was negatively correlated with axial length in most grids ($P < 0.05$).

Conclusions: Choroidal changes could be quantified using ultra-widefield SS-OCTA. Choroidal thinning with increasing axial length indicated regional differences in eyes with myopia, which were most evident in the macular area. Decreased CSHL vessel density with increasing axial length also indicated regional differences in eyes with myopia.

Translational Relevance: This study explored choroidal changes with a wider field of view than has been currently available.

Introduction

Myopia is a common eye condition that can cause visual impairment and poses a significant public health burden.[1–3] In 2020, the prevalence of myopia and high myopia increased to 34% and 5.4% of the global population, respectively.[3] Myopia has a higher prevalence in Asian populations, especially in China.[1,2] This is particularly alarming because myopia-related changes indicate choroidal abnormalities.[4,5] These changes may be associated with vision impairment and indicative of future progression of this disease or the need for active intervention.[6] Choroid, the major vascular layer in the eye, plays an important role in the pathogenesis of myopia.[7] A better understanding of the choroidal changes in myopia is important for preventing and controlling structural changes in myopia.

In recent years, optical coherence tomography angiography (OCTA) has provided growing evidence of vascular dysfunction in myopia. Spectral-domain (SD)-OCTA was the most widely distributed and deployed modality in these studies.[8,9] However, swept-source (SS)-OCTA offers higher speed imaging and higher sensitivity than SD-OCT.[10] SS-OCTA has been used previously to assess choroidal capillary plexus in the macular area of myopia on 3 × 3-mm or 6 × 6-mm scans.[11,12] Moon et al.[13] increased the scanning area to 12 mm × 12 mm and found changes

in choroidal thickness in the peripheral area in eyes with myopia. Choroidal thinning was most evident in the macular area, with no statistically significant decrease in peripheral fields.[13] On 3 × 3-mm scans, a longer axial length was associated with thinner choroid in eyes with myopia, but there was no association between axial length and choroidal thinning on widefield scans.[13] This suggests that choroidal thinning shows regional differences in eyes with myopia. The association between axial length and vessel density in various choroidal layers in peripheral fields has not been adequately studied.

Ultra-widefield imaging, which shows features of the region anterior to the vortex vein ampullae in all four quadrants, can provide a more complete understanding of the nuanced variations in eyes with myopia.[14] Optos confocal scanning laser ophthalmoscopy allows 200° fundus photography in a single image capture.[15] Moriyama et al.[16] assessed the unique features of the posterior vortex veins in eyes with high myopia using ultra-widefield indocyanine green angiography (ICGA), but they could not quantify choroidal changes. More information on the peripheral and deeper choroidal changes could help elucidate the potential role of the choroid in myopia progression.[17]

Compared with previous studies, this study provides greater insight into choroidal changes, including choroidal thickness and vessel indices in different layers, in patients with myopia by using ultra-widefield SS-OCTA with a scanning area of 24 mm × 20 mm.

Materials and Methods

Study Subjects

This cross-sectional, observational study was conducted at The First Affiliated Hospital of Anhui Medical University. This study was approved by the institutional committee on medical ethics and adhered to the tenets of the Declaration of Helsinki. Volunteers with myopia, as certified by their history and ophthalmic examination, were recruited and informed of the purpose of the study. All participants underwent comprehensive ophthalmic examinations, including best-corrected visual acuity (BCVA) evaluation, diopters (D), slit-lamp biomicroscopy of the anterior segment, fundus examination, intraocular pressure, axial length, and ultra-widefield SS-OCTA. The exclusion criteria were as follows: (1) systemic disease; (2) other ocular diseases, such as cataract, glaucoma, or retinal diseases; (3) history of intraocular surgery, laser surgery, or refractive surgery; (4) ocular injury; (5) eyes with a scan quality index of OCTA images of <6; and (6) diopters of astigmatism > 2 D. The diopters were collected and converted to spherical equivalent (SE), which was the spherical dioptric power plus half of the cylindrical dioptric power. The IOLMaster 5.0 (Carl Zeiss Meditec, Jena, Germany) was used to measure axial length. Eyes were categorized as having low myopia (LM; refractive error with SE ≥ −3.00 D), moderate myopia (MM; refractive error of −6.0 D < SE ≤ −3.0D), or high myopia (HM; refractive error with SE ≤ −6 D) based on the SE.[18]

Ultra-Widefield SS-OCTA

All participants were imaged using a 400-kHz SS-OCTA instrument (TowardPi BMizar; TowardPi Medical Technology, Beijing, China) with 400,000 scans per second. It utilizes a swept-source vertical-cavity surface-emitting laser (VCSEL) with a wavelength of 1060 nm, providing a transverse resolution of 10 µm and in-depth resolution (optical) of 3.8 µm in tissue. Each OCT volume was 2560 pixels deep × 1536 pixels wide × 1280 B-scans which corresponded to nominal physical dimensions of 6 mm deep × 24 mm wide × 20 mm. The 24 × 20-mm rectangle scans, corresponding to a 120° angular field of view, centered on the fovea were acquired by two trained photographers. These examinations were performed between 8:00 AM and 11:00 AM. They were performed in the normal pupil state to prevent the circadian rhythm and anti-cholinergic drugs from affecting the outcomes. All images were manually reviewed to exclude those with severe artifacts that could affect the analysis. Severe artifacts were defined as occurring when >10% of the area of the superficial capillary plexus image contained motion artifacts, segmentation failure occurred, and the capillary network could not be easily distinguished from the background signal scan centration.[19]

Image Analysis

Images of the choroidal capillary plexus (CCP) and choroidal Sattler's and Haller's layers (CSHL) were generated automatically using built-in software. The instrument automatically outlined the boundaries of the CCP extending from the Bruch's membrane to 29 µm below the Bruch's membrane (Fig. 1A) and those of CSHL extending from 29 µm below the Bruch's membrane to the choroid–sclera interface (Fig. 1B). In some cases, the error in automatic segmentation was manually corrected for the entire scan volume. We chose 3 × 3 grids (comprised of nine rectangles: tempo-superior, superior, nasal-superior, tempo, macular, optic disc, tempo-inferior, inferior, and nasal-inferior) with a total area of 17 mm × 17 mm to analyze

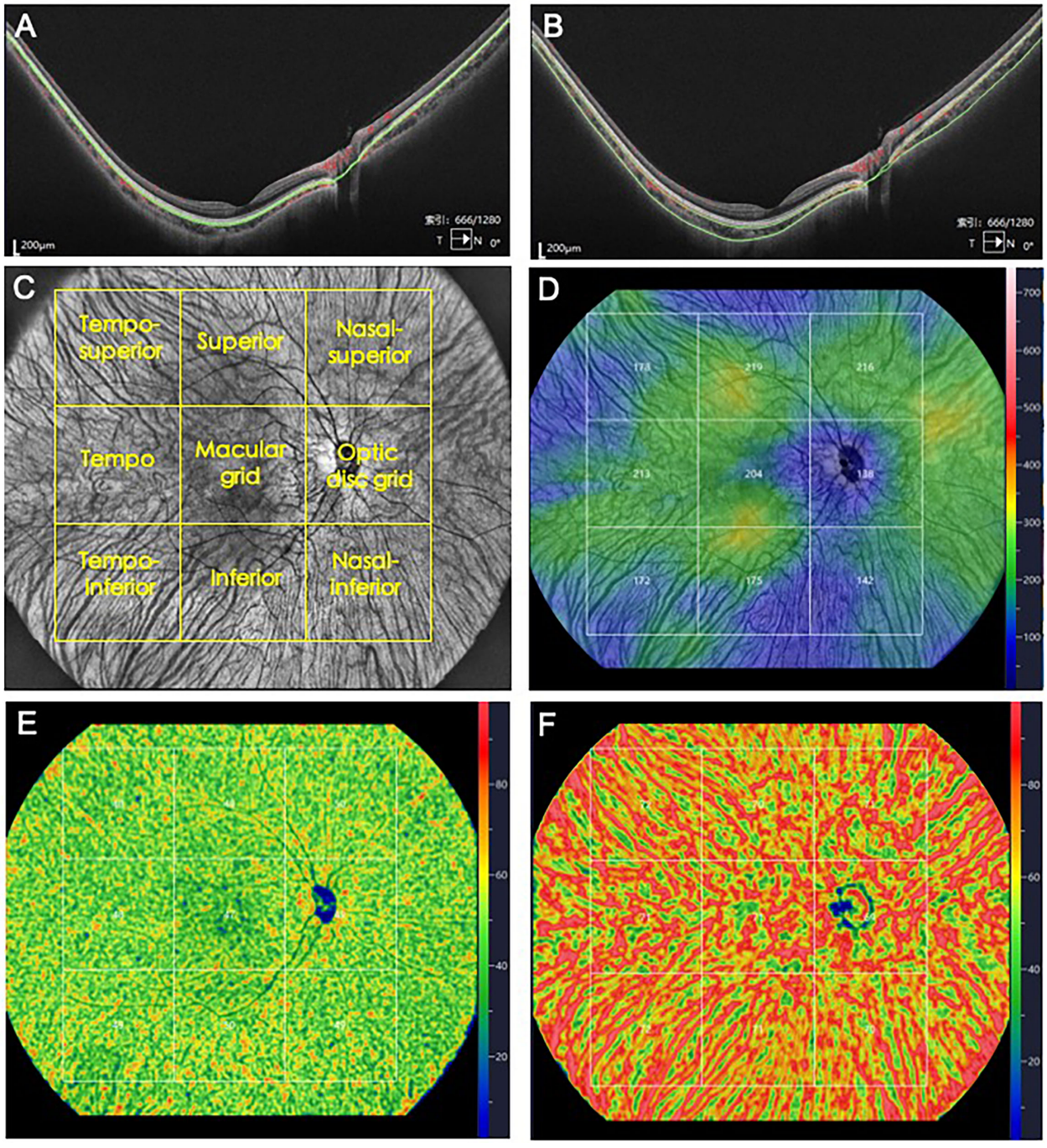

Figure 1. (A) Representative B-scan shows the boundaries of the CCP extending from the Bruch's membrane to 29 µm below the Bruch's membrane. (B) Representative B-scan shows boundaries of the CSHL extending from 29 µm below the Bruch's membrane to the choroid–sclera interface. (C) OCTA en face image showing 3 × 3 grids (comprised of nine rectangles: tempo-superior, superior, nasal-superior, tempo, macular, optic disc, tempo-inferior, inferior, and nasal-inferior) with a total area of 17 mm × 17 mm that were chosen to analyze the parameters of the retina and choroid. (D) Representative OCTA en face image showing choroidal thickness in myopia using a color map. (E, F) Representative OCTA scans showing vessel density of the CCP (E) and CSHL (F) in myopia using color maps.

the parameters of the choroid (Fig. 1C). All images were manually evaluated to confirm proper placement of the 3 × 3 grids, with the macular fovea placed centrally and the optic disc placed in the nasal grid (Fig. 1C). Choroidal thickness (Fig. 1D), CCP vessel density (Fig. 1E), and CSHL vessel density (Fig. 1F) in the nine rectangles were obtained using the built-in software algorithm. Vessel density is the percentage of

the observed pixel area depicting blood flow (%). These vessel metrics were corrected by inputting the actual axial length values into the software to adjust for ocular magnifications.

Statistical Analysis

The distribution of continuous numerical data was checked using the Kolmogorov–Smirnov test. Continuous numerical data are reported as median and interquartile range (IQR, 25th–75th percentile). Classified data are reported as percentages. The repeatability of studied parameters between two photographers was analyzed using the intraclass correlation coefficient (ICC). The studied parameters were compared between groups using Kruskal–Wallis H or χ^2 tests. Least-significant difference and Duncan's tests for multiple comparisons were used to compare values between groups. Pearson's or Spearman's correlation analysis was used to estimate relationships among the studied parameters depending on their distribution. Regression lines were plotted for a straightforward comparison. Significance was determined at $P < 0.05$. All analyses were performed using SPSS Statistics 21.0 (IBM, Chicago, IL).

Results

Demographics and Clinical Characteristics

A total of 105 eyes of 105 participants were enrolled in this study, including 31 eyes with LM, 38 with MM, and 36 with HM. The demographic and clinical characteristics of the patients are shown in Table 1.

Repeatability Analysis of Choroidal Thickness and Vascular Metrics Obtained by Two Different Photographers

The ICCs for choroidal thickness and vascular metrics obtained by the two different photographers are shown in Table 2. The results for CCP vessel density (ICC > 0.5) showed good repeatability, and those of

Table 1. Demographic and Clinical Characteristics of Eyes Included in the Study

	LM	MM	HM	*P*
Patients, *n*	31	38	36	—
Eyes, *n*	31	38	36	—
Asian ethnicity, *n*	31	38	36	—
Gender, *n* (%)				
Female	22 (71)	31 (82)	26 (72)	0.522
Male	9 (29)	7 (18)	10 (28)	—
Age (y), median (25th–75th percentile)	21.0 (19.0–23.0)	21.0 (19.0–23.3)	20.0 (19.0–24.0)	0.711
BCVA (logMAR), median (25th–75th percentile)	0 (0–0.1)	0 (0–0.1)	0 (0–0.1)	0.843
IOP (mmHg), median (25th–75th percentile)	15.7 (13.7–17.0)	15.4 (13.3–16.6)	14.9 (13.4–15.6)	0.355
Scan quality index, median (25th–75th percentile)	8.0 (7.0–8.0)	7.0 (7.0–8.0)	7.5 (7.0–8.0)	0.662

Significant $P < 0.05$ values are highlighted in bold.

Table 2. Repeatability Analysis of Choroidal Thickness and Vascular Metrics Between Two Photographers

	Choroidal Thickness (μm)		CCP Vessel Density (%)		CSHL Vessel Density (%)	
Grid	ICC	*P*	ICC	*P*	ICC	*P*
Tempo-superior	0.99	**<0.001**	0.71	**<0.001**	0.92	**<0.001**
Superior	0.97	**<0.001**	0.59	**<0.001**	0.83	**<0.001**
Nasal-superior	0.99	**<0.001**	0.70	**<0.001**	0.93	**<0.001**
Tempo	0.97	**<0.001**	0.74	**<0.001**	0.90	**<0.001**
Macular	0.98	**<0.001**	0.70	**<0.001**	0.88	**<0.001**
Optic disc	0.96	**<0.001**	0.65	**<0.001**	0.97	**<0.001**
Tempo-inferior	0.98	**<0.001**	0.58	**<0.001**	0.97	**<0.001**
Inferior	0.99	**<0.001**	0.64	**<0.001**	0.86	**<0.001**
Nasal-inferior	0.98	**<0.001**	0.67	**<0.001**	0.96	**<0.001**

Significant $P < 0.05$ values are highlighted in bold.

choroidal thickness and CSHL vessel density (ICC > 0.8) showed excellent repeatability between both photographers (all $P < 0.001$). The mean values of the measurements performed by the two photographers were used for subsequent statistical analysis.

Comparison of Choroidal Thickness and Vascular Metrics in Eyes With Different Degrees of Myopia

We found significant differences in choroidal thickness in most grids ($P < 0.01$) among the LM, MM, and HM groups, except in the nasal-superior ($P = 0.262$) and optic disc ($P = 0.335$) grids (Table 3). Post hoc multiple comparisons showed that choroidal thickness in the HM group was significantly less than that in the LM group in most grids ($P < 0.001$) (Fig. 2A), except in the nasal-superior and optic disc grids. The choroidal thickness in the MM group was significantly less than that in the LM group in some grids ($P < 0.01$) (Fig. 2A), except in the nasal-superior, tempo, nasal-inferior, and optic disc grids. Further, the choroidal thickness in the HM group was less than that in the MM group only in the macular grid ($P < 0.01$) (Fig. 2A).

There was no statistical difference in the vessel density of CCP among the LM, MM, and HM groups in all grids (all $P > 0.05$) (Table 3). The CSHL vessel density showed significant differences among the LM, MM, and HM groups in most grids ($P < 0.05$), except in the tempo-superior ($P = 0.176$), nasal-superior ($P = 0.786$), and optic disc ($P = 0.127$) grids (Table 3). Post hoc multiple comparisons showed that the HM group had significantly lower CSHL vessel density than did the LM group in most grids ($P < 0.05$) (Fig. 2B),

Table 3. Comparison of Choroidal Thickness and Vascular Metrics in Eyes With Different Degrees of Myopia

Parameter	LM	MM	HM	*P*
Choroidal thickness (μm) by grid, median (25th–75th percentile)				
Tempo-superior	262.5 (228.5–279.0)	224.0 (203.8–262.5)	212.0 (188.3–258.4)	**0.003**
Superior	263.0 (226.0–315.5)	229.3 (193.4–268.0)	212.5 (189.6–246.0)	**<0.001**
Nasal-superior	234.0 (187.0–269.5)	229.5 (174.8–259.4)	206.5 (166.8–243.1)	0.262
Tempo	259.0 (235.5–302.0)	238.8 (217.5–296.4)	232.5 (196.8–259.9)	**0.006**
Macular	270.5 (244.5–335.5)	240.0 (204.4–288.1)	214.8 (183.4–227.8)	**<0.001**
Optic disc	175.0 (133.5–210.0)	172.3 (141.0–208.4)	160.0 (123.5–190.5)	0.335
Tempo-inferior	223.0 (187.0–262.0)	185.8 (155.8–217.5)	160.8 (138.6–207.6)	**<0.001**
Inferior	192.0 (167.5–262.5)	163.0 (131.6–197.9)	156.3 (134.6–176.9)	**<0.001**
Nasal-inferior	140.5 (126.5–172.0)	126.0 (106.4–153.8)	123.3 (98.3–136.3)	**0.002**
CCP vessel density (%) by grid, median (25th–75th percentile)				
Tempo-superior	49.0 (48.0–49.5)	49.0 (48.4–49.5)	49.0 (48.0–50.0)	0.910
Superior	49.0 (48.5–49.5)	49.0 (48.4–49.5)	49.3 (48.5–50.0)	0.356
Nasal-superior	50.0 (49.0–50.5)	49.5 (48.5–50.0)	49.5 (49.0–50.0)	0.219
Tempo	48.5 (48.0–49.0)	48.0 (47.5–48.5)	48.0 (47.5–49.0)	0.431
Macular	47.0 (46.0–47.5)	46.5 (45.9–47.1)	46.5 (46.0–47.5)	0.235
Optic disc	49.0 (48.0–49.5)	48.0 (47.0–49.0)	48.5 (47.5–49.0)	0.231
Tempo-inferior	48.5 (47.5–49.0)	48.5 (47.5–49.0)	48.5 (47.5–49.0)	0.809
Inferior	49.5 (48.5–50.0)	49.0 (48.4–49.5)	48.8 (48.0–49.9)	0.234
Nasal-inferior	49.0 (48.0–50.0)	49.0 (48.0–49.5)	49.0 (48.1–49.5)	0.838
CSHL vessel density (%) by grid, median (25th–75th percentile)				
Tempo-superior	73.0 (72.0–74.0)	72.5 (72.0–73.0)	72.0 (70.6–73.5)	0.176
Superior	70.5 (70.0–72.0)	70.0 (69.5–71.0)	70.0 (69.0–71.0)	**0.005**
Nasal-superior	71.0 (70.0–72.0)	71.0 (70.4–72.0)	71.5 (70.0–72.4)	0.786
Tempo	72.5 (72.0–73.5)	72.0 (71.0–73.0)	71.5 (71.0–73.0)	**0.035**
Macular	72.0 (71.0–72.5)	71.0 (70.4–72.0)	71.0 (70.0–71.9)	**0.016**
Optic disc	69.5 (67.0–71.0)	69.3 (67.0–70.5)	68.0 (65.6–70.0)	0.127
Tempo-inferior	73.5 (72.5–74.0)	72.5 (71.5–74.0)	71.5 (69.6–74.0)	**0.005**
Inferior	71.5 (70.0–72.0)	70.5 (69.5–71.5)	70.3 (68.0–71.0)	**0.017**
Nasal-inferior	70.5 (69.5–71.5)	69.5 (68.8–70.6)	69.0 (65.8–70.0)	**<0.001**

Significant $P < 0.05$ values are highlighted in bold.

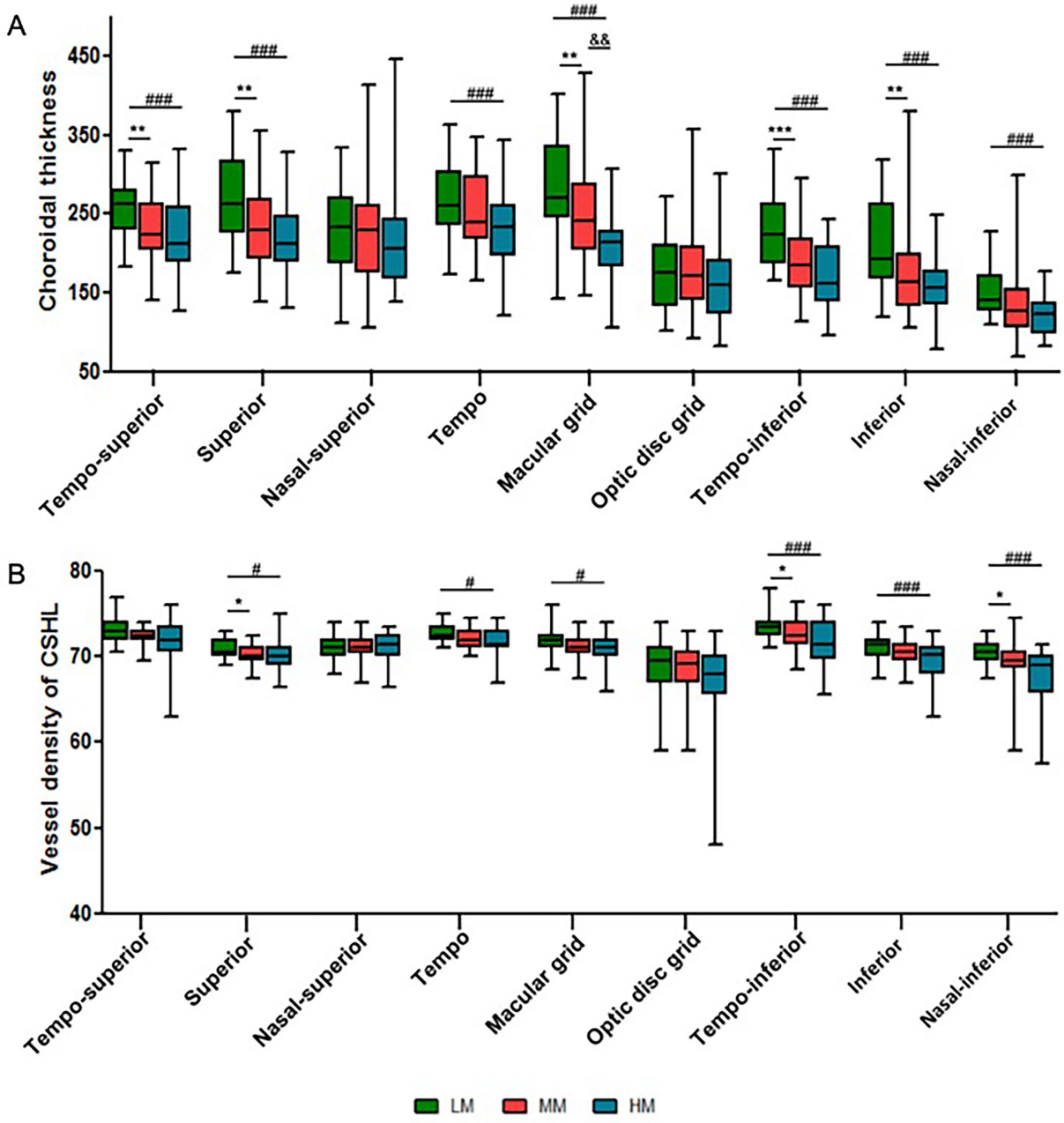

Figure 2. (A) Boxplots of average thickness of choroid in different areas, separated by the study group. (B) Boxplots of average values of CSHL vessel density in different areas, separated by study group: LM versus MM ($^{*}P < 0.05$, $^{**}P \leq 0.01$, $^{***}P \leq 0.001$); LM versus HM ($^{\#}P < 0.05$, $^{\#\#\#}P \leq 0.001$); and MM versus HM ($^{\&\&}P \leq 0.01$).

except in the tempo-superior, nasal-superior, and optic disc grids.

Correlations of the Choroidal Thickness and Vascular Metrics With Axial Length

Pearson's correlation indicated that thinner choroid was correlated with longer axial length in most grids ($P < 0.05$) but not in the nasal-superior ($P = 0.255$) or optic disc ($P = 0.375$) grids (Table 4). The vessel density of CCP was not correlated with axial length in any grids (all $P > 0.05$) (Table 4). However, lower CSHL vessel density was significantly correlated with a longer axial length in most grids ($P < 0.05$), except in the tempo-superior ($P = 0.726$), nasal-superior (P = 0.685), and optic disc ($P = 0.171$) grids (Table 4). Regression lines showed choroidal thinning with increasing axial length was most evident in the macular grid ($\beta = -22.55$, $P < 0.001$) (Fig. 3).

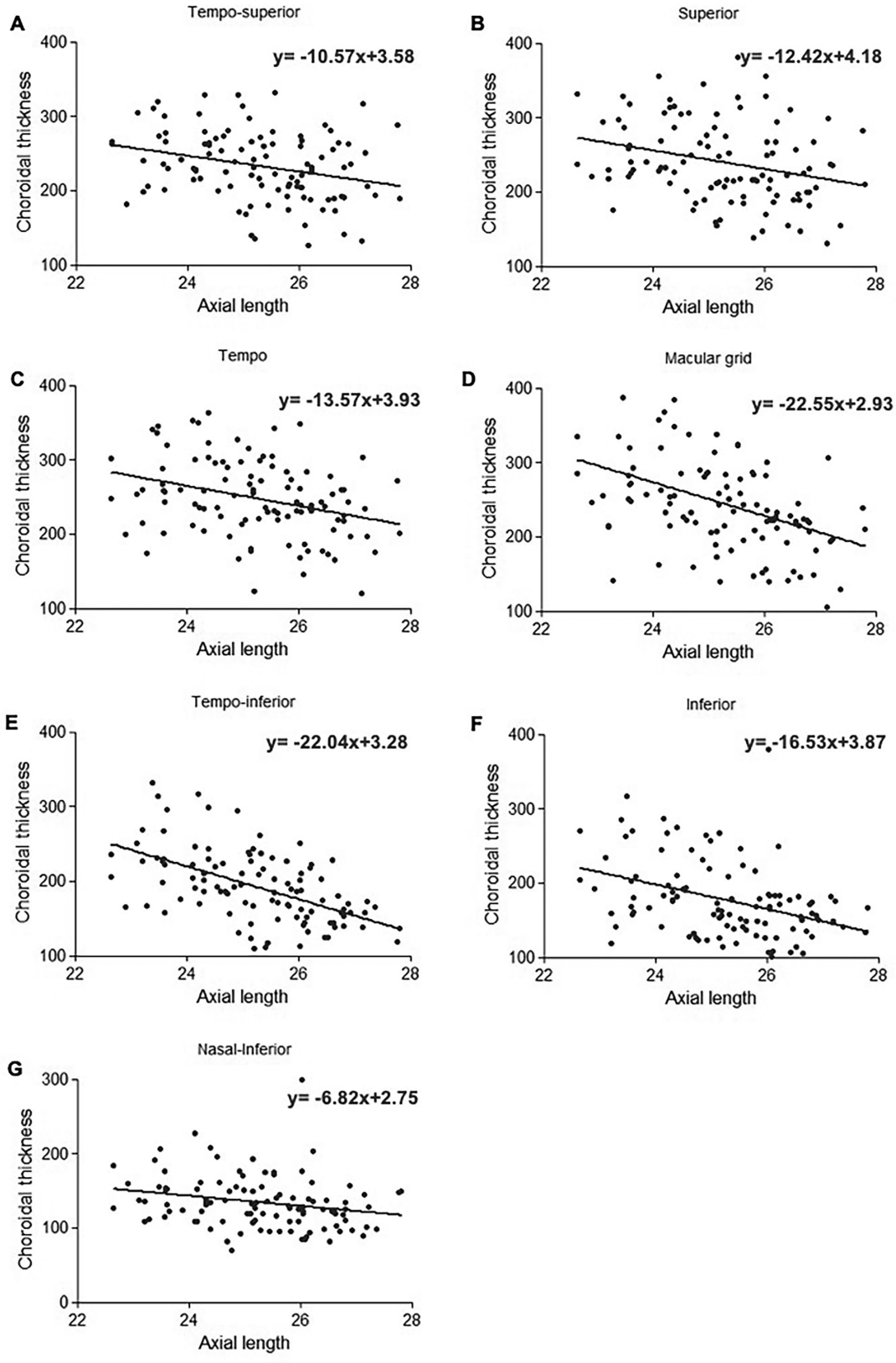

Figure 3. Scatterplots of choroidal thickness and axial length in eyes with myopia. (A) Choroidal thickness in the tempo-superior grid. (B) Choroidal thickness in the superior grid. (C) Choroidal thickness in the tempo grid. (D) Choroidal thickness in the macular grid. (E) Choroidal thickness in the tempo-interior grid. (F) Choroidal thickness in the inferior grid. (G) Choroidal thickness in the nasal-inferior grid.

Table 4. Correlation Analysis Between Choroidal Thickness and Vascular Metrics (Dependent Variables) and Axial Length (Independent Variable)

	Choroidal Thickness (μm)		CCP Vessel Density (%)		CSHL Vessel Density (%)	
Grid	Correlation Coefficient	*P*	Correlation Coefficient	*P*	Correlation Coefficient	*P*
Tempo-superior	−0.291	**0.003**	0.137	0.164	−0.035	0.726
Superior	−0.312	**0.001**	0.136	0.166	−0.273	**0.005**
Nasal-superior	−0.112	0.255	−0.087	0.378	0.040	0.685
Tempo	−0.328	**0.001**	−0.095	0.336	−0.225	**0.021**
Macular	−0.470	**<0.001**	−0.014	0.891	−0.207	**0.034**
Optic disc	−0.087	0.375	−0.060	0.544	−0.135	0.171
Tempo-inferior	−0.565	**<0.001**	−0.054	0.587	−0.447	**<0.001**
Inferior	−0.404	**<0.001**	−0.066	0.502	−0.302	**0.002**
Nasal-inferior	−0.289	**0.003**	−0.041	0.675	−0.331	**0.001**

Significant $P < 0.05$ values are highlighted in bold.

Discussion

In this study, we analyzed and quantified structural and vascular changes in various choroidal layers in eyes with myopia using ultra-widefield SS-OCTA with a wide view field up to 120°. In HM, we found a significant decrease in the choroidal thickness in most grids, except in the nasal-superior and optic disc grids. The CSHL vessel density showed a significant decrease in most grids in HM, except in the tempo-superior, nasal-superior, and optic disc grids. Choroidal thickness was negatively correlated with axial length in most grids but not in the nasal-superior or optic disc grids. Choroidal thinning was most evident in the macular grid. The CSHL vessel density was negatively correlated with axial length in most grids.

OCTA has played an important role in evaluating retinal microvascular metrics in clinical and research settings in the last decade.[20–22] Due to scattering by the retinal pigment epithelium, imaging of the vascular flow from various choroidal layers using OCTA is challenging. According to a recent study, ultra-widefield SS-OCTA could provide improved visualization of the CCP and CSHL, similar to that during histopathological examination.[23] The reproducibility of OCTA is essential to determine its reliability for utilization. Wider scans result in a lower transverse resolution, and, subsequently, higher coefficients of variation could make choroidal parameters difficult to capture.[24,25] However, use of a VCSEL, 100-nm bandwidth, a set of large-diameter lenses, 128-Hz eye tracking rate, and 15-second average acquisition time in the ultra-widefield OCTA made it possible to obtain a 24 × 20-mm rectangular scan while still maintaining a lateral resolution of 10 μm.[23] SS-OCT imaging at 1060 nm allows better tissue penetration with minimal water dispersion and higher quality and deeper imaging of the outer retina, choroidal tissue morphology, and vascular plexus.[23] Thus, we quantified vessel density with larger scan areas of the CCP and CSHL using this technology. We analyzed the repeatability of the results of choroidal thickness and vascular metrics obtained by two different photographers. The results of ultra-widefield SS-OCTA demonstrated high reproducibility in assessing choroidal thickness measurements and vascular metrics.

Our results showed decreasing choroidal thickness in most grids with increasing severity of myopia, except in the nasal-superior and optic disc grids. Pearson's correlation indicated that a thinner choroid was correlated with longer axial length in most grids, but not in the nasal-superior or optic disc grids. A previous study reported that choroidal thinning during accommodation is most pronounced within the temporal region but not the subfoveal region.[26] Harb et al.[27] found thinner choroids in eyes with longer axial lengths at all locations except at 2250 μm temporal to the fovea. Although the measurement of choroidal thickness in these studies was limited to a 3-mm B-scan around the fovea, the results showed regional differences in choroidal thinning in eyes with myopia.[26,27] According to the most widely accepted theory of pathogenesis, the mechanical stretching caused by axial elongation results in choroidal thinning. Tian et al.[26] and Vincent et al.[28] reported that choroidal thinning related to myopia is only partially explained by simple passive choroidal thinning with axial elongation.

Previous studies have demonstrated choroidal thinning in myopia that is associated with the progression of myopic macular degeneration.[29–31] We found that choroidal thinning was most evident in the

macular grid according to the nine rectangles on the ultra-widefield SS-OCTA scans. The change in the choroidal thickness in the macular grid was consistent with the findings of Moon et al.,[13] who observed thinner choroid associated with longer axial length in the central macula on 3 × 3-mm scans. The sharper decrease in the macular choroidal thickness in eyes with myopia supports the hypothesis that axial elongation leads to stretching of the posterior pole of the choroid.[32]

The secondary purpose of the study was to evaluate the effect of myopia on choroidal vascular indices in different layers in myopia. Choroid is predominantly composed of blood vessels and is one of the tissues with the highest blood flow in the body.[33,34] Agrawal et al.[35] found that vascular area is a predominant segment influencing choroidal thickness in the normal population. The choroidal vessels can be differentiated into three layers: capillary plexus in the innermost layer, Sattler's layer with medium vessels in the middle, and Haller's layer with large vessels in the outer.[33] The ultra-widefield SS-OCTA used in this study allows wider non-invasive quantitative assessment of choroidal vascular indices in the different layers. Al-Sheikh et al.[36] and Su et al.[37] both reported that the area of flow deficit in the choriocapillaris increased in eyes with greater myopia; however, no significant difference in the vessel density of CCP was found among the different degrees of myopia in any grid in this study. The choriocapillaris was derived with a slab 10 µm thick starting 31 µm deep to the retinal pigment epithelium–Bruch's membrane in previous studies.[36,37] The instrument used in our study automatically outlined the boundaries of the CCP extending from the Bruch's membrane to 29 µm below the Bruch's membrane. On the other hand, eyes with high myopia included in the previous studies were more severely affected than those included in our study.[36,37] Alshareef et al.[38] reported that medium choroidal vessel thickness decreased significantly in non-pathological eyes with myopia compared to that of healthy subjects. A histological study of myopia and an ICGA study also reported a reduction in large choroidal vessels,[39,40] which is consistent with our finding of a significant decrease in the vessel density in CSHL. Lower CSHL vessel density was significantly correlated with longer axial length in most grids. Thus, decreased CSHL vessel density with increasing axial length also indicated regional differences in eyes with myopia. The contraction of nonvascular smooth muscle cells in the choroid, especially behind the fovea, may thin the choroid and inhibit its thickening caused by expansion of the lacunae.[41] Intrinsic choroidal neurons, especially those behind the central retina, may also modulate choroidal blood flow.[34]

Recent research has indicated that choroidal thinning, possibly related to hypoxia, causes pathological myopia. Ei Matri et al.[42] found that eyes with HM with choroidal neovascularization had significantly thinner subfoveal choroid than eyes without choroidal neovascularization. Longitudinal studies on the relationship between choroidal thinning and choroidal blood flow are needed to develop new treatment approaches for pathological myopia.

There are several limitations that must be considered in our study. First, we did not include eyes with extremely high myopia because of low vision and poor fixation. Some parameters, such as CCP vessel density, lacked significant correlation with axial length, which may be attributed to the limited sample rather than a real lack of associations. Second, we found that the optic disc was placed in different grids in different eyes when using 3 × 3 grids with a total area of 24 mm × 20 mm. This can lead to incomparability and poor reproducibility of the findings due to anatomical differences at different sites. Thus, we chose 3 × 3 grids with a total area of 17 mm × 17 mm to analyze the parameters. All images were manually evaluated to confirm the proper placement of 3 × 3 grids with an optic disc placed in the nasal grid; however, this method resulted in a lack of choroidal information obtained from the nasal periphery in this study. Finally, project artifacts such as the shadow from the superficial layer on the choroidal layers are not removed fully from the OCTA volume.

Conclusions

In summary, we quantified the vascular and structural changes in the choroid based on the degree of myopia using ultra-widefield SS-OCTA. Choroidal thinning with increasing axial length showed regional differences in myopic eyes, which were most evident in the macular area. Decreased CSHL vessel density with increasing axial length also indicated regional differences in myopic eyes. Further investigations may help elucidate the pathogenesis of myopia.

Acknowledgments

Disclosure: **J. Gao**, None; **C. Rao**, None; **F. Li**, None; **L. Liu**, None; **K. Liu**, None

* JG and CR contributed equally to this work and should be considered co-first authors.

References

1. You QS, Wu LJ, Duan JL, et al. Prevalence of myopia in school children in greater Beijing: the Beijing Childhood Eye Study. *Acta Ophthalmol.* 2014;92(5):e398–e406.
2. Koh V, Yang A, Saw SM, et al. Differences in prevalence of refractive errors in young Asian males in Singapore between 1996–1997 and 2009–2010. *Ophthalmic Epidemiol.* 2014;21(4):247–255.
3. Holden BA, Fricke TR, Wilson DA, et al. Global prevalence of myopia and high myopia and temporal trends from 2000 through 2050. *Ophthalmology.* 2016;123(5):1036–1042.
4. Ikuno Y. Overview of the complications of high myopia. *Retina.* 2017;37(12):2347–2351.
5. Liu R, Guo X, Xiao O, et al. Diffuse chorioretinal atrophy in Chinese high myopia: the ZOC-BHVI High Myopia Cohort Study. *Retina.* 2020;40(2):241–248.
6. Shih Y-F, Ho T-C, Hsiao C-K, Lin LL-K. Visual outcomes for high myopic patients with or without myopic maculopathy: a 10 year follow up study. *Br J Ophthalmol.* 2006;90(5):546–550.
7. Xiong S, He X, Zhang BO, et al. Changes in choroidal thickness varied by age and refraction in children and adolescents: a 1-year longitudinal study. *Am J Ophthalmol.* 2020;213:46–56.
8. Spaide RF, Fujimoto JG, Waheed NK, Sadda SR, Staurenghi G. Optical coherence tomography angiography. *Prog Retin Eye Res.* 2018;64:1–55.
9. Jiang Y, Lou S, Li Y, Chen Y, Lu TC. High myopia and macular vascular density: an optical coherence tomography angiography study. *BMC Ophthalmol.* 2021;21(1):407.
10. Mastropasqua R, Viggiano P, Borrelli E, et al. In vivo mapping of the choriocapillaris in high myopia: a widefield swept source optical coherence tomography angiography. *Sci Rep.* 2019;9(1):18932.
11. Wong CW, Matsumura S, Htoon HM, et al. Assessment of the macular microvasculature in high myopes with swept source optical coherence tomographic angiography. *Front Med (Lausanne).* 2021;8:619767.
12. Dai Y, Xin C, Zhang Q, et al. Impact of ocular magnification on retinal and choriocapillaris blood flow quantification in myopia with swept-source optical coherence tomography angiography. *Quant Imaging Med Surg.* 2021;11(3):948–956.
13. Moon JY, Garg I, Cui Y, et al. Wide-field swept-source optical coherence tomography angiography in the assessment of retinal microvasculature and choroidal thickness in patients with myopia. *Br J Ophthalmol.* 2023;107(1):102–108.
14. Ludwig CA, Moon J, Garg I, Miller JB. Ultra-widefield imaging for evaluation of the myopic eye. *Semin Ophthalmol.* 2021;36(4):185–190.
15. Patel SN, Shi A, Wibbelsman TD, Klufas MA. Ultra-widefield retinal imaging: an update on recent advances. *Ther Adv Ophthalmol.* 2020;12:2515841419899495.
16. Moriyama M, Cao K, Ogata S, Ohno-Matsui K. Detection of posterior vortex veins in eyes with pathologic myopia by ultra-widefield indocyanine green angiography. *Br J Ophthalmol.* 2017;101(9):1179–1184.
17. Zhu Y, Cui Y, Wang JC, et al. Different scan protocols affect the detection rates of diabetic retinopathy lesions by wide-field swept-source optical coherence tomography angiography. *Am J Ophthalmol.* 2020; 215:72–80.
18. Tai ELM, Ling JL, Gan EH, Adil H, Wan-Hazabbah W-H. Comparison of peripapillary retinal nerve fiber layer thickness between myopia severity groups and controls. *Int J Ophthalmol.* 2018;11(2):274–278.
19. Fenner BJ, Tan GSW, Tan ACS, Yeo IYS, Wong TY, Cheung GCM. Identification of imaging features that determine quality and repeatability of retinal capillary plexus density measurements in OCT angiography. *Br J Ophthalmol.* 2018;102(4):509–514.
20. Robbins CB, Thompson AC, Bhullar PK, et al. Characterization of retinal microvascular and choroidal structural changes in Parkinson disease. *JAMA Ophthalmol.* 2021;139(2):182–188.
21. Lonngi M, Velez FG, Tsui I, et al. Spectral-domain optical coherence tomographic angiography in children with amblyopia. *JAMA Ophthalmol.* 2017;135(10):1086–1091.
22. Ashraf M, Sampani K, Rageh A, Silva PS, Aiello LP, Sun JK. Interaction between the distribution of diabetic retinopathy lesions and the association of optical coherence tomography angiography scans with diabetic retinopathy severity. *JAMA Ophthalmol.* 2020;138(12):1291–1297.
23. Xuan Y, Chang Q, Zhang Y, et al. Clinical observation of choroidal osteoma using swept-source optical coherence tomography and optical coherence tomography angiography. *Appl Sci.* 2022;12:4472.
24. You Q, Freeman WR, Weinreb RN, et al. Reproducibility of vessel density measurement with optical coherence tomography angiography in eyes with and without retinopathy. *Retina.* 2017;37(8):1475–1482.

25. Carpineto P, Mastropasqua R, Marchini G, Toto L, Di Nicola M, Di Antonio L. Reproducibility and repeatability of foveal avascular zone measurements in healthy subjects by optical coherence tomography angiography. *Br J Ophthalmol.* 2016;100(5):671–676.
26. Tian F, Zheng D, Zhang J, et al. Choroidal and retinal thickness and axial eye elongation in Chinese junior students. *Invest Ophthalmol Vis Sci.* 2021;62(9):26.
27. Harb E, Hyman L, Gwiazda J, et al. Choroidal thickness profiles in myopic eyes of young adults in the Correction of Myopia Evaluation Trial cohort. *Am J Ophthalmol.* 2015;160(1):62–71.
28. Vincent SJ, Collins MJ, Read SA, Garney LG. Retinal and choroidal thickness in myopic anisometropia. *Invest Ophthalmol Vis Sci.* 2013;54(4): 2445–2456.
29. Wu H, Zhang G, Shen M, et al. Assessment of choroidal vascularity and choriocapillaris blood perfusion in anisomyopic adults by SS-OCT/OCTA. *Invest Ophthalmol Vis Sci.* 2021; 62(1):8.
30. Wu Q, Chen Q, Lin B, et al. Relationships among retinal/choroidal thickness, retinal microvascular network and visual field in high myopia. *Acta Ophthalmol.* 2020;98(6):e709–e714.
31. Lundberg K, Vestergaard AH, Jacobsen N, et al. Choroidal thickness and myopia in relation to physical activity – the CHAMPS Eye Study. *Acta Ophthalmol.* 2018;96(4):371–378.
32. Troilo D, Nickla DL, Wildsoet CF. Choroidal thickness changes during altered eye growth and refractive state in a primate. *Invest Ophthalmol Vis Sci.* 2000;41(6):1249–1258.
33. Alm A, Bill A. Ocular and optic nerve blood flow at normal and increased intraocular pressures in monkeys (*Macaca irus*): a study with radioactively labelled microspheres including flow determinations in brain and some other tissues. *Exp Eye Res.* 1973;15(1):15–19.
34. Nickla DL, Wallman J. The multifunctional choroid. *Prog Retin Eye Res.* 2010;29(2):144–168.
35. Agrawal R, Gupta P, Tan K-A, Cheung CMG, Wong T-Y, Cheng C-Y. Choroidal vascularity index as a measure of vascular status of the choroid: measurements in healthy eyes from a population-based study. *Sci Rep.* 2016;6(1):21090.
36. Al-Sheikh M, Phasukkijwatana N, Dolz-Marco R, et al. Quantitative OCT angiography of the retinal microvasculature and the choriocapillaris in myopic eyes. *Invest Ophthalmol Vis Sci.* 2017;58(4):2063–2069.
37. Su L, Ji YS, Tong N, et al. Quantitative assessment of the retinal microvasculature and choriocapillaris in myopic patients using swept-source optical coherence tomography angiography. *Graefes Arch Clin Exp Ophthalmol.* 2020;258(6):1173–1180.
38. Alshareef RA, Khuthaila MK, Januwada M, Goud A, Ferrara D, Chhablani J. Choroidal vascular analysis in myopic eyes: evidence of foveal medium vessel layer thinning. *Int J Retina Vitreous.* 2017;3(1):28.
39. Grossniklaus HE, Green WR. Pathologic findings in pathologic myopia. *Retina.* 1992;12(2):127–133.
40. Quaranta M, Arnold J, Coscas G, et al. Indocyanine green angiographic features of pathologic myopia. *Am J Ophthalmol.* 1996;122(5):663–671.
41. May CA. Non-vascular smooth muscle cells in the human choroid: distribution, development and further characterization. *J Anat.* 2005;207(4):381–390.
42. El Matri L, Bouladi M, Chebil A, et al. Choroidal thickness measurement in highly myopic eyes using SD-OCT. *Ophthalmic Surg Lasers Imaging.* 2012;43(6 suppl):S38–S43.